

# Sizes and shapes of very heavy nuclei in high- $K$ states

M. Palczewski<sup>1</sup>, P. Jachimowicz<sup>2</sup>, and M. Kowal<sup>1\*</sup>

<sup>1</sup> *National Centre for Nuclear Research, Pasteura 7, 02-093 Warsaw, Poland and*

<sup>2</sup> *Institute of Physics, University of Zielona Góra, Z. Szafrana 4a, 65-516 Zielona Góra, Poland*

(Dated: June 4, 2020)

We have investigated shapes and sizes of selected two- and four-quasiparticle high- $K$  states in nobelium and rutherfordium isotopes within the microscopic-macroscopic model with the deformed Woods-Saxon potential. Excited nuclear configurations were obtained by blocking single-particle states lying close to the Fermi level. Their energies and deformations were found by the four-dimensional energy minimization over shape variables. We have selected the most promising candidates for  $K$ -isomers by analyzing the isotopic dependence of excitation energies, and compared our results to available experimental data. We calculated differences in quadrupole moments and charge radii between nuclei in their high- $K$  and ground states and found their quite different pattern for four-quasiparticle states in neighbouring No and Rf isotopes. The leading role of the quadrupole and hexadecapole deformations as well as the importance of higher rank symmetries is also discussed. The current development of laser techniques and the resulting ability to measure discussed effects in near future are the motivation of our study.

PACS numbers: 21.10.-k, 21.60.-n, 27.90.+b

## I. INTRODUCTION

Shapes and sizes of atomic nuclei are their primary characteristics. Their study acquires a flavour of novelty for very heavy nuclear systems for which still relatively little is known. Quite recently, a development of laser spectroscopy methods, improving measurements of hyperfine splitting and isotope shifts [1–6], has been achieved. The laser-based spectroscopic techniques allowed to perform model-independent and direct measurement of basic quantities related to nuclear shapes: electric quadrupole moments and mean-square charge radii, for very heavy nuclei. Those measurements provide not only important and new information on nuclear shapes and sizes but also provide a test for theoretical models as they are sensitive not only to the bulk properties but also to the single-particle spectrum/configurations. Quite recently, such laser-based data on ground-states of <sup>252,253,254</sup>No were discussed and published by Raeder et al. [7]. Nobelium is so far the heaviest element in which these quantities could be measured.

An interesting question is what are sizes and shapes of the high- $K$  isomers which frequently occur in these nuclei. In particular, does a multi-quasiparticle excitation increase or decrease the size of a nuclear system relative to that of the ground state? A pioneering experiment in which the collinear laser spectroscopy was applied to the four-quasiparticle (qp) isomeric state in <sup>178</sup>Hf $f^{m2}$  pointed out that the change in nuclear mean-square charge radius is  $\delta\langle r^2 \rangle = -0.059(9)fm^2$  [8]. This means that nuclear size of the isomer is significantly smaller than that of the ground state. How the shape of very heavy multi-quasiparticle isomers changes along the isotopic chains

is another interesting question. Motivated by the mentioned unprecedented development in accuracy of the laser measuring techniques, here we would like to provide some answers to those questions.

A review of the current experimental knowledge on isomers in the heaviest nuclei can be found in [9–13], while theoretical overview based on the Nilsson - Strutinsky approach was given in [14]. As follows from the cited works, for nuclei close to nobelium and rutherfordium the occurrence of high- $K$ , low-lying isomeric states seems to be very likely due to the predicted existence of the deformed shell gaps at  $Z = 100$  and  $N = 152$  [15].

There is another extremely interesting aspect of such research: the size of a nucleus, whether in the ground or isomeric state, is closely related to physics of the alpha decay. This is of particular importance in the context of a search for hindrance mechanisms in this decay. Recently, we predicted [16] a quite strong hindrance against alpha decay for four-qp states:  $K^\pi = 20^+$  and/or  $19^+$ , and two-quasiproton state:  $K^\pi = 10^-$  in darmstadtium nuclei and for some odd and odd-odd superheavy nuclei [17]. Together with their relatively low excitation, this suggests a possibility that they could be isomers with an extra stability.

Although a link of such quantities as the alpha-decay energy  $Q_\alpha$  and half-life with the size and shape of the nucleus is not always obvious, intuitively one may expect some relationships. i) The size of a nucleus will have effect on the pre-formation probability of the alpha cluster inside nucleus. The probability of alpha particle formation should be different in its periphery. ii) The action integral used to estimate alpha half-life is strongly dependent on the turning points which are in turn very much dependent on the nuclear radius. iii) For an isomer,  $Q_\alpha$  energy available in the emission process may change significantly, and that will, in a non-direct way, affect rather considerably the integration limits (see previous point),

---

\*Electronic address: [michal.kowal@ncbj.gov.pl](mailto:michal.kowal@ncbj.gov.pl)

and so the whole tunneling process through such effectively changed potential barrier.

The main goal of this paper is to provide predictions for sizes and shapes of very heavy nuclei in high- $K$  states. Relevant quantities: electric quadrupole moments and nuclear charge radii are calculated within the MM model. Since s.p. wave functions in such a model are used only to calculate shell corrections, they are not suited for the quantities of interest for this work. Therefore we use the liquid-drop model formulas which allow to calculate both, the quadrupole moment and the mean-square radius as the functions of only deformations. It has to be emphasized, that this approach seems a approximation and its usefulness for high- $K$  configuration will depend on how well it compares with experimental data.

## II. THE METHOD

To obtain energies and deformations for the ground (gs) and excited (ex) states the microscopic-macroscopic (MM) method is used. In the frame of this approach microscopic energy is calculated via applying the Strutinski shell and pairing correction [18] method to single particle levels of the deformed Woods-Saxon potential [19]. The  $n_p = 450$  lowest proton levels and  $n_n = 550$  lowest neutron levels from the  $N_{max} = 19$  lowest shells of the deformed harmonic oscillator are taken into account in the diagonalization procedure. Standard values of  $\hbar\omega_0 = 41/A^{1/3}$  MeV for the oscillator energy and  $\gamma = 1.2\hbar\omega_0$  for the Strutinski smearing parameter  $\gamma$ , and the sixth-order correction polynomial are used in the calculation of the shell correction. For the macroscopic part we used the Yukawa plus exponential model [20] with parameters specified in [21]. Thus, all parameter values are kept exactly the same as in all recent applications of the model to heavy and superheavy nuclei, e.g., [16, 22–30].

In the considered region of nobelium nuclei, the ground- as well as excited states are expected to be well deformed and axially- and reflection-symmetric. This means that intrinsic parity of states is well defined and that  $K$  is a "good" quantum number. Admittedly, this assumption cannot be exact for high- $K$  states, in which the time-reversal breaking effects are expected to break the axial symmetry to some degree.

In the present study we used four deformation parameters within the standard  $\beta$  parametrization. The nuclear radius vector  $R(\theta, \phi)$  is parameterized via spherical harmonics  $Y_{\lambda\mu}(\theta, \phi)$  as follows:

$$R(\theta) = cR_0[1 + \sum_{\lambda=2,4,6,8} \beta_{\lambda 0} Y_{\lambda 0}(\theta)], \quad (1)$$

where  $c$  is the volume-fixing factor depending on deformation and  $R_0$  is the radius of a spherical nucleus taken as:  $R_0 = 1.16 \cdot A^{1/3} fm$ .

To find the gs minima, i.e. energies and shapes, the four-dimensional energy minimization over  $\beta_{20} - \beta_{80}$  is

performed using the gradient method. Such minimization is repeated dozens of times for a given nucleus with different starting values of deformations. To obtain excitation energies, after blocking of a chosen configuration, a similar minimization procedure, over the same deformations, was performed once again.

We would like to emphasize that the used MM model, among all existing, offers not only an excellent agreement with existing data in the region of super-heavy nuclei (concerning: masses, deformations [22],  $Q_\alpha$ -energies [28], first and second fission barriers in actinides [26], etc.) but also, what is even more important for spectroscopic studies, provides at the same time two prominent enough energetic shell gaps at  $Z = 100$  in protons and  $N = 152$  in neutrons. Without this, it seems, no realistic predictions for  $K$ -isomers in this region of nuclei were possible.

## III. RESULTS AND DISCUSSION

### A. Excitation energies of the selected 2- and 4-qp high- $K$ , possibly isomeric states

Promising candidates for metastable isomers are energetically low-lying high- $K$  states. The natural candidates are configurations built by particles blocked on levels in close proximity to the Fermi energy. In the region of No and Rf nuclei such characteristic multi-quasiparticle configurations are as follows:

- two-proton (2-qp isomer):  
 $K^\pi = \pi^2 8^- \{ \pi 7/2^- [514] \otimes \pi 9/2^+ [624] \},$
- two-neutron (2-qp isomer):  
 $K^\pi = \nu^2 8^- \{ \nu 7/2^+ [624] \otimes \nu 9/2^- [734] \},$
- two-proton plus two-neutron (4-qp isomer), build on two configurations above:  
 $K^\pi = \pi^2 \nu^2 16^+ \{ \pi^2 8^- \otimes \nu^2 8^- \}.$

They will be the subject of our further considerations concerning their sizes and shapes. However, first we discuss their excitation energies. As explained earlier, for a given nucleus, from independently performed minimizations, we obtained deformations and energies of ground states and the constrained minima for selected few-qp configurations. The energy difference between these minima gives the excitation energy of a certain multi-qp configuration:

$$E^* = \Delta E = E^{ex} - E^{gs}. \quad (2)$$

Those energies are shown for isotopic chains of No in Fig. 1, and Rf, in Fig. 2. As can be seen, excitation energies of two-proton qp state (red dots) are very low-lying for both elements, what makes them promising candidates for 2-quasiproton isomers in the whole range of considered neutron numbers  $N$ . One can also see that

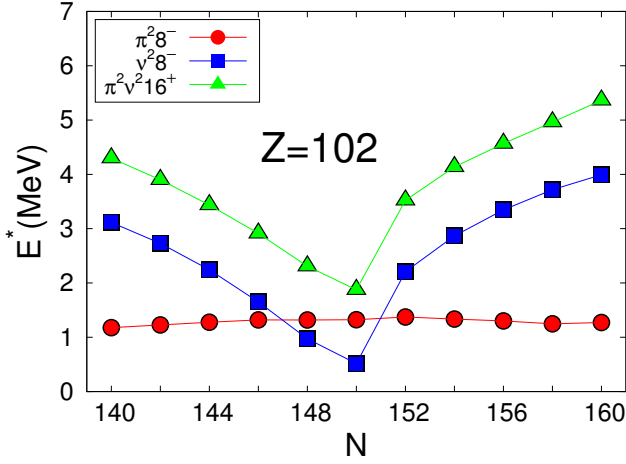


FIG. 1: Calculated excitation energies (2) for multi-qp high- $K$  states in No isotopes. Configurations:  $\pi^2 8^- = \{\pi 7/2^- [514] \otimes \pi 9/2^+ [624]\}$ ,  $\nu^2 8^- = \{\nu 7/2^+ [624] \otimes \nu 9/2^- [734]\}$ ,  $\pi^2 \nu^2 16^+ = \{\pi^2 8^- \otimes \nu^2 8^-\}$ . The lines are drawn to guide an eye.

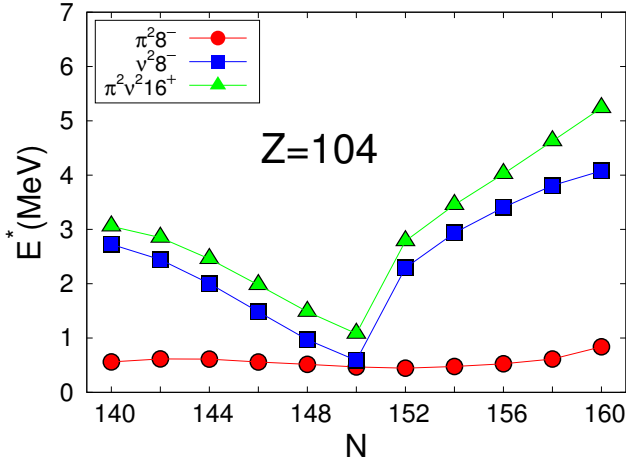


FIG. 2: The same as in Fig. 1, but in Rf isotopes.

the extremely low  $E^*$  values for  $\pi^2 8^-$  state are obtained in Rf isotopes, and that in both, No and Rf elements, excitation energies of such 2-quasiproton configuration show very weak isotopic dependence.

From these figures one can choose the best candidates for two-quasineutron isomers (blue dots). As we clearly see for both considered elements, the lowest excitation energies of the  $\nu^2 8^-$  configuration occur for  $N = 150$ . Moreover, in  $^{250}\text{No}$  (Fig. 1), such two-quasineutron state lies much lower than the two-quasiproton one, while in  $^{248,250}\text{No}$  as well as in  $^{254}\text{Rf}$  both corresponding  $E^*$  values are roughly similar. In all remaining cases, the proton 2-qp configuration always lies below the 2-quasineutron state.

The  $N$ -dependence of these two (proton and neutron) energies allows a prediction of the most favorable four-quasiparticle  $\pi^2 \nu^2 16^+$  candidates. As can be seen in

Figs. 1 and 2 in green, such 4-qp high- $K$  isomeric state can appear most likely in  $^{252}\text{No}$  and  $^{254}\text{Rf}$  because of the smallest excitation energy.

It seems interesting to make a similar analysis for specific neutron shells  $N = 150$  and  $152$  for different elements from this area. Such isotonic chains for  $Z = 100 - 112$  are shown in Figs. 3 and 4 for  $N = 152$  and  $N = 152$ , respectively. This time we see very low lying two-neutron configuration  $\nu^2 8^-$  practically for all taken nuclei with neutron number  $N = 150$ . This confirms the previous observation that the best candidate isomers is  $^{254}\text{Rf}$ . Excitation of two-neutrons from the closed  $N = 152$  shell costs more energy as seen in Fig. 4 in which this excitation is shown (in blue). This behavior of neutrons basically blocks the possibility for the creation of any 4-qp isomers for all nuclei possessing such number of neutrons. However, one can notice a very promising candidate for two-proton isomer in  $^{256}\text{Rf}$ . From Fig. 4 one can not still completely exclude possible formation of the two-proton isomer in  $^{254}\text{No}$  and  $^{258}\text{Sg}$ . Similar conclusion about the two-proton state can be drawn from Fig. 3 and concerns  $^{252}\text{No}$  and  $^{256}\text{Sg}$ .

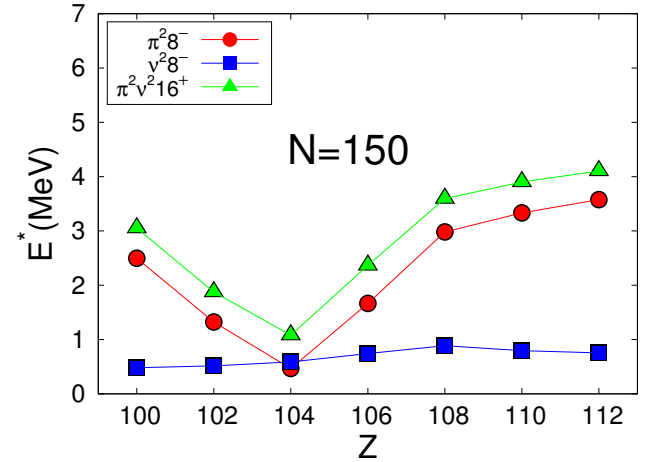


FIG. 3: The same as in Fig. 1, but for  $N = 150$  isotones in the range from fermium to copernicium.

## B. Obtained excitation energies vs experimental data

Before discussing shapes let us discuss the compliance of the obtained  $E^*$  values with experimental data. As already mentioned, those configurations are relatively well-known for  $K$ -isomers in nobelium and rutherfordium isotopes investigated here (see the data set collected in Table 2 in [11]).

We start our comparison with  $^{254}\text{No}$  for which the first observations of excited state postulated as the isomeric one were carried out already almost 50 years ago [31]. Observed band characterised by  $E^* = 0.988 \text{ MeV}$  [32] was assigned there to the two-quasiproton  $K^\pi = 3^+$

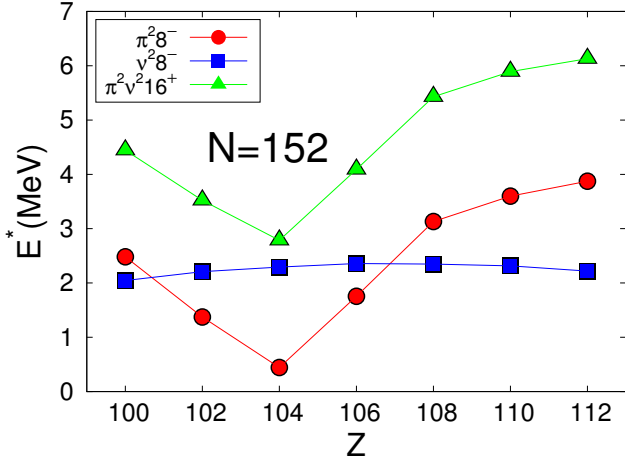


FIG. 4: The same as in Fig. 1, but for  $N = 152$  isotones in the range from fermium to copernicium.

state. This and other experimental observations can be compared with our theoretical results for  $^{254}\text{No}$ , shown in Fig. 5.

Let us note that in Fig. 5 all possible combinations of two-quasiparticle configurations for protons (red colour) and neutrons (blue colour) that one can obtain from the deformed Woods-Saxon model after 4-dimensional minimization over all  $\beta_{\lambda 0}$  in (1) and lying at energy lower than  $E^* = 1.5 \text{ MeV}$  has been shown. One can see e.g. that the  $3^+$  state  $\{\pi 1/2^- [521] \otimes \pi 7/2^- [514]\}$  has the excitation energy a little below  $0.7 \text{ MeV}$  and it is the lowest obtained possible two-quasiproton configuration. There is also another low-lying proton state, not very distant ( $\sim 200 \text{ keV}$ ) from it, namely:  $K^\pi = 5^-$  state:  $\{\pi 1/2^- [521] \otimes \pi 9/2^+ [624]\}$  and this one more closely matches the measured energy  $E^* = 0.988 \text{ keV}$  [32].

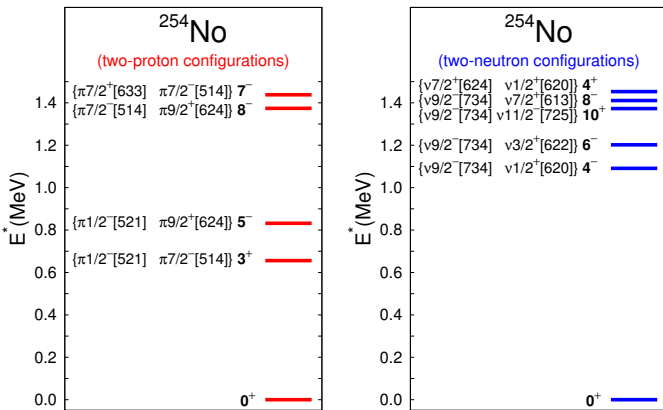


FIG. 5: Calculations of  $^{254}\text{No}$  two-quasiproton states (left) and two-quasineutron states (right) with excitation energy  $E^* \leq 1.5 \text{ MeV}$ .

The difficulty in assigning the appropriate configuration is even more apparent for the next important candi-

date for isomeric configuration, namely  $K^\pi = 8^-$ , which is located around  $E^* \approx 1.4 \text{ MeV}$  in both proton and neutron spectra of most MM models. Exact predictions of excitation energies in various microscopic-macroscopic approaches for such two-quasiparticle  $K^\pi = 8^-$  states are collected in Table III of [11]. One can see that all of them are in the range  $\langle 1.1 \div 1.5 \rangle \text{ MeV}$ , while the exact measured values of  $E^*$  (in  $\text{keV}$ ) are the following: 1293 [33, 34], 1296 [32], 1295(2) [35], 1297(2) [36]. In our calculations the following two-proton configuration:  $\{\pi 7/2^- [514] \otimes \pi 9/2^+ [624]\}$  with  $E^* \approx 1.4 \text{ MeV}$  (left side of Fig. 5) may be assigned to the experimental excitation of this  $K^\pi = 8^-$  state. On the other hand, looking on the right side of Fig. 5, where excitation energies of two-neutron quasiparticle states are presented, one can notice another just as likely  $K^\pi = 8^-$  configuration and attribute it as:  $\{\nu 9/2^- [734] \otimes \nu 7/2^+ [613]\}$  at the same energy. Interestingly, one can also see in our neutron spectrum another high spin state  $K^\pi = 10^-$  near it, this time as a result of adding the following two-neutron components:  $\{\nu 9/2^- [734] \otimes \nu 11/2^- [725]\}$ .

Second candidate which one can consult with the obtained values of excitation energies is  $^{252}\text{No}$ . The experimental excitation energy for the  $K$ -isomer in this nucleus is  $1.25 \text{ MeV}$  [37, 38] with the half-life  $T_{1/2} = 109(6) \text{ ms}$ . According to Fig. 1, the state that best suits this energy is the two-quasiproton excitation  $\pi^2 8^- = \{\pi 7/2^- [514] \otimes \pi 9/2^+ [624]\}$  with  $E^*$  about  $1.3 \text{ MeV}$  in our calculation. Two neutron state considered earlier in  $^{252}\text{No}$ , namely:  $\{\nu 9/2^- [734] \otimes \nu 7/2^+ [613]\}$ , this time is much higher in energy ( $E^* = 1.97 \text{ MeV}$ ). However, as discussed in the previous section and shown in Fig. 1, there is another neutron configuration:  $\{\nu 9/2^- [734] \otimes \nu 7/2^+ [624]\}$ , the most favorable to form  $K$ -isomer. Its energy is two times smaller than reported in the experiment.

Theoretical predictions for two-quasiparticle states in  $^{252}\text{No}$ , depending on their mutual combinations, give excitation energies in the range  $\langle 0.9 \div 1.4 \rangle \text{ MeV}$ . Predictions for the lowest  $E^*$  usually come from the Woods-Saxon model with the Lipkin-Nogami version of including pair correlations [39], while the highest excitations are predicted e.g. within the quasiparticle phonon model [40], namely  $E^* = 1.300 \text{ MeV}$  for  $\nu^2 8^- = \{\nu 9/2^- [734] \otimes \nu 7/2^+ [624]\}$  and  $E^* = 1.336 \text{ MeV}$  for  $\pi^2 8^- = \{\pi 7/2^- [514] \otimes \pi 9/2^+ [624]\}$ .

Next comparison can be done for  $^{250}\text{No}$  for which quite recently stability of the high- $K$  isomer was investigated by Kallunkathariyil et al. [41]. In the previous study [42] a tentative assignment of the isomeric state was:  $K^\pi = \nu^2 6^+$ , with the following neutron components:  $\{\nu 5/2^+ [622] \otimes \nu 7/2^+ [624]\}$ . The experimental energy is not known. Our calculations fully support such assignment as this configuration is clearly low laying:  $E^* \approx 0.6 \text{ MeV}$  in the case of our already weak pairing interaction within the BCS formalism. Higher states (with energies in  $\text{MeV}$ ) are collected in Table I. Also the modified two-center shell model predicts this  $K^\pi = \nu^2 6^+$  state as the most likely  $K$ -isomer ( $E^*$  about  $1.2 \text{ MeV}$ ).

TABLE I: Specification of excited states in  $^{250}\text{No}$ 

$\pi/\nu K^\pi$	Configuration	$E^*$ (MeV)
$\nu^2 6^+$	$\{\nu 5/2^+[622] \otimes \nu 7/2^+[624]\}$	0.57
$\nu^2 7^-$	$\{\nu 5/2^+[622] \otimes \pi 9/2^-[734]\}$	0.76
$\nu^2 8^-$	$\{\nu 7/2^+[624] \otimes \pi 9/2^-[734]\}$	0.97
$\nu^2 4^+$	$\{\nu 7/2^+[624] \otimes \pi 1/2^+[631]\}$	1.10
$\nu^2 7^-$	$\{\nu 7/2^-[743] \otimes \pi 7/2^+[624]\}$	1.21
$\nu^2 5^-$	$\{\nu 1/2^+[631] \otimes \pi 9/2^-[734]\}$	1.24
$\nu^2 8^+$	$\{\nu 7/2^-[743] \otimes \pi 9/2^-[734]\}$	1.34

Liu et al. [43], selects this configuration as the favored one for the two-quasiparticle isomer in  $^{250}\text{No}$  as well (with energy  $E^* = 0.83 \text{ MeV}$ ).

Finally we would like to compare our data to the recent measurement in  $^{254}\text{Rf}$ . Using digital electronic, under vacuum conditions at the Fragment Mass Analyser at Argonne, two signals suspected of 2-qp configurations:  $\pi^2 8^- = \{\nu 9/2^-[734] \otimes \nu 7/2^+[624]\}$  or  $\pi^2 8^- = \{\pi 7/2^-[514] \otimes \pi 9/2^+[624]\}$  were registered. The 4-qp isomeric state, likely:  $\{\pi^2 8^- \otimes \nu^2 8^-\}$ , involving one of those, has been found by David et al. [44]. These are extremely low-lying states according to our calculations, see Fig. 2. Possible underestimate of  $E^*$  in our calculations has its source in the BCS treatment of pairing: the blocking procedure within this method induces a too large reduction in the pairing gap for multi-quasiparticle states and causes an underestimate in their excitation energies. Therefore our  $E^*$  may tend to be lower than the corresponding experimental excitations. One possibility to avoid such deficiency would be to assume a stronger pairing interaction for considered multi-qp configurations. However, because such modification will not affect the sizes and shapes of studied multi-quasiparticle configurations and (according to our tests) only systematically increases calculated  $E^*$ , we decided to keep all our BCS parameters without any adjustment.

### C. Role of the high rank deformations

The MM method used here allows to examine step by step the role of deformation parameters of the higher order. Patyk and Sobiczewski in [45, 46] noted a wider shell gap around  $Z = 100$  and  $N = 150$  after the inclusion of  $\beta_{60}$  in their definition of the nuclear radius, which gave them much better agreement with existing experimental data. Recently, an effect of the deformation  $\beta_{60}$  on high- $K$  isomer properties in superheavy nuclei has been discussed by Liu et al. [47]. Here, we use even one more deformation -  $\beta_{80}$ . In this subsection we would like to discuss changes in deformation parameters  $\beta_{20}, \beta_{40}, \beta_{60}, \beta_{80}$ , along isotopic chains, both for the ground states as well for high- $K$  configurations. As an example of such an excited configuration we will consider the mentioned earlier:  $\pi^2 \nu^2 16^+ = \{\pi^2 8^- \otimes \nu^2 8^-\}$ , build on the following two-

quasiproton:  $\pi^2 8^- = \{7/2^-[514] \otimes 9/2^+[624]\}$  and two-quasineutron:  $\nu^2 8^- = \{7/2^+[624] \otimes 9/2^-[734]\}$  excitations. For simplicity, this 4-qp state is indicated in Figs. 6-9 as:  $16^+$ .

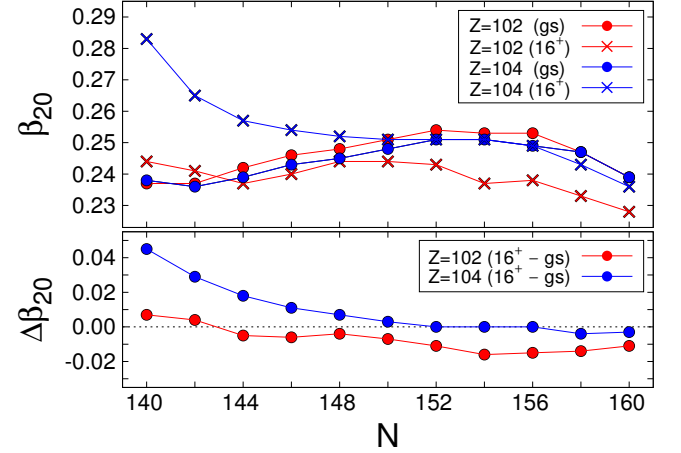


FIG. 6: Upper panel: Values of the deformation parameter  $\beta_{20}$  in the ground (gs) and excited 4-qp states  $\pi^2 \nu^2 16^+ = \{\pi^2 8^- \otimes \nu^2 8^-\}$  ( $16^+$ ), for No and Rf isotopes (red and blue color, respectively). Bottom panel: Differences between  $\beta_{20}$  values in the  $16^+$  and gs states for two isotopic chains:  $Z = 102$  and  $Z = 104$  (red and blue color, respectively).

The quadrupole deformation ( $\beta_{20}$ ) effect on energy is the largest - Fig. 6. One can see on the top panel of this figure that No nuclei (red filled circles) are in most cases slightly more quadrupole deformed at the ground states than the Rf nuclei (blue filled circles). First and foremost, one can see systematically different behavior of this parameter for the two tested isotopic chains in excited states. Except two cases:  $^{242}\text{No}$  and  $^{244}\text{No}$ , in all considered nobelium nuclei the quadrupole deformation is smaller in excited states compared to the ground states. However such differences, namely:  $\Delta\beta_{20} = \beta_{20}^{ex} - \beta_{20}^{gs}$ , are not large as shown on the bottom panel of Fig. 6 (red circles), where it can be seen that they grow insignificantly for heavier isotopes. For Rf isotopes lighter than  $^{254}\text{Rf}$ , the differences (blue circles on the bottom panel in Fig. 6), are clearly increasing as the number of neutrons decreases. In the extreme case, the deformation difference of considered excited state  $\pi^2 \nu^2 16^+$  with respect to the gs reaches up to 20 percent. Quadrupole deformations of the excited state for heavier Rf nuclei are actually the same as those at the ground state.

The isotopic behavior of hexadecapole deformation for No and Rf isotopes is shown in Fig. 7. Also this time the ground states values of this shape variable are systematically and clearly higher for No than for Rf. In contrast to what we observed for the quadrupole in both chains the course of variation  $\Delta\beta_{40} = \beta_{40}^{ex} - \beta_{40}^{gs}$  is now similar i.e.: their values for excited 4-qp configurations are negative for lighter nuclear systems and very close to zero for the heavier ones ( $N > 148$ ). This is reflected on

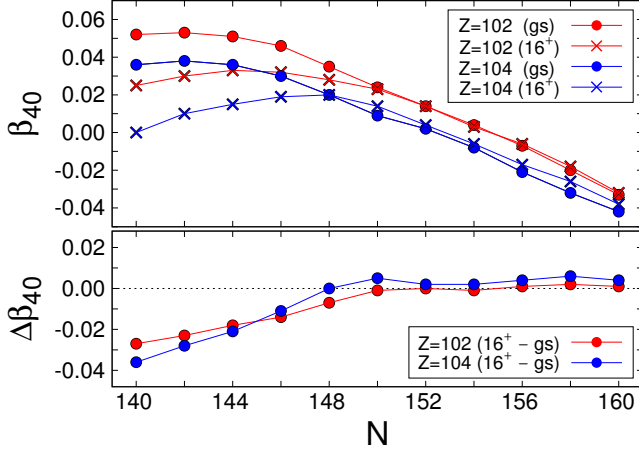


FIG. 7: The same as in Fig. 6, but for the deformation parameter  $\beta_{40}$ .

bottom panel in the Fig. 7. We would like to emphasize that relative changes of this hexadecapole deformation for considered 4-qp state are really enormous for lighter isotopes.

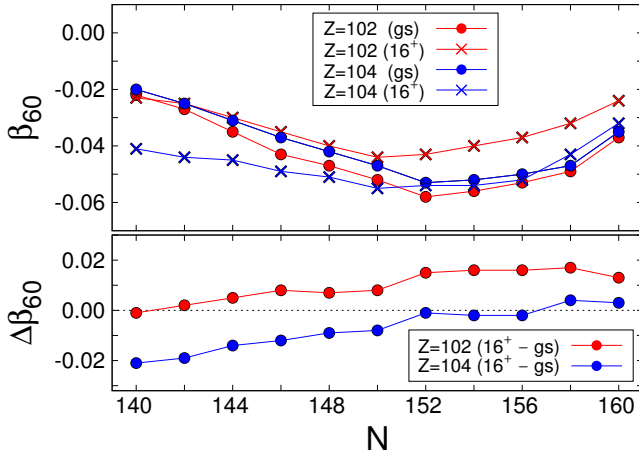


FIG. 8: The same as in Fig. 6, but for the deformation parameter  $\beta_{60}$ .

Yet another behavior is revealed by  $\beta_{60}$  parameter what has been shown in Fig. 8. In the sense of the absolute value of this variable nobelium nuclei are almost always much more deformed at the ground states than at the considered  $\pi^2\nu^216^+$  excited state (top panel of Fig. 8). In rutherfordium nuclei the situation is a little different, namely: for  $N < 152$  excited nuclei are visibly less deformed in this direction compared to the ground states. For  $N \geq 152$  the  $\beta_{60}$  deformation of considered high- $K$  configuration are quite similar to the corresponding ground state configurations. The differences,  $\Delta\beta_{60} = \beta_{60}^{ex} - \beta_{60}^{gs}$ , of this parameter in the  $N$  chains are shown on the bottom panel of Fig. 8.

For completeness, we also plotted the deformations  $\beta_{80}^{gs}$

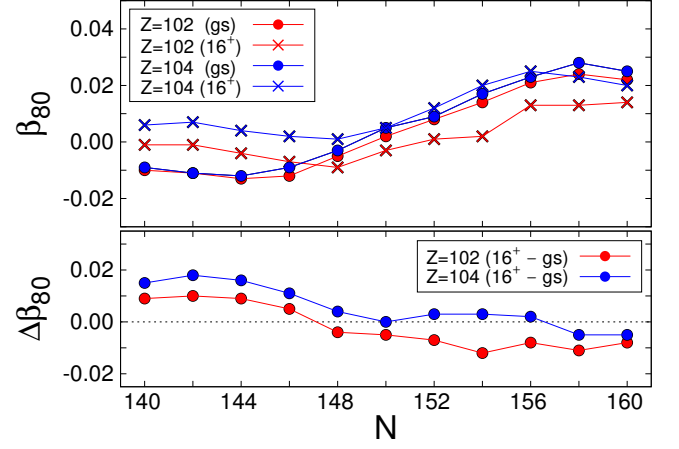


FIG. 9: The same as in Fig. 6, but for the deformation parameter  $\beta_{80}$ .

and  $\beta_{80}^{ex}$  as the function of the neutron number  $N$  (top panel of Fig. 9). Of course, these changes are rather not as important as the previous ones. However, it can be seen that the values of this deformation parameter for both chains are almost the same in ground states. Also the isotopic variation of  $\Delta\beta_{80}$  is similar (the bottom panel of Fig. 9).

Finally, in Fig. 10, the shapes for  $^{244}\text{Rf}$  nucleus corresponding to its ground (on black) as well to excited high- $K$  state  $\pi^2\nu^216^+$  (green color), are shown. This is exactly the same 4-qp configuration as considered previously in Figs. 6-9. In the scale of the obtained values of deformations, the differences between this two shapes are not very significant. However, in the scale of energy these differences are very clear and, for example in this particular nucleus, the energy difference (i.e. excitation energy  $E^*$ ) is about 3 MeV.

#### D. Electric quadrupole moments

A deviation of the proton distribution from sphericity is characterized by the electric quadrupole moment. Assuming a uniform distribution of the charge  $Ze$  within a sharp, deformed nuclear surface, i.e. neglecting the diffuseness of the nuclear surface, one obtains the intrinsic electric quadrupole moment:

$$Q_{20}^{ex/gs} = \frac{3Ze}{4\pi r_0^3} \int_0^{R(\theta)} r^2(\theta) P_{20}(\theta) d^3r. \quad (3)$$

In the leading order,  $Q_{20}$  is proportional to  $\beta_{20}$ , but other deformations are also included in the above formula. Within the MM model, we disregard possible differences between the proton and neutron deformations. The moment (3) is calculated in the intrinsic frame, while measurements are performed in the laboratory frame. The usually assumed transformation between the two



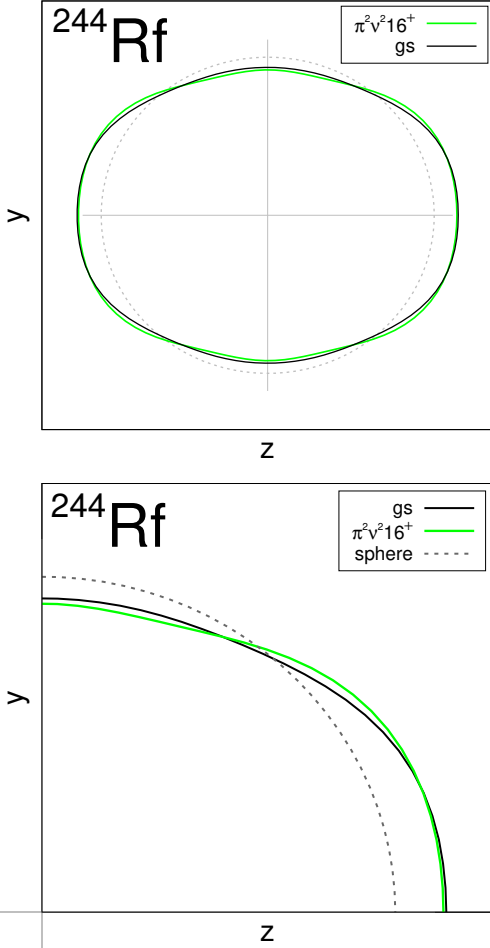


FIG. 10: Cut of a sample shape in the  $y - z$  plane for  $^{244}\text{Rf}$ . Green line - calculation for 4-qp excited state ( $\pi^2\nu^216^+$ ); black line - calculation for ground state (gs).

neglects the Coriolis effects. This is substantiated for high- $K$  states in well deformed nuclei, in which  $K$  is good quantum number. In this strong coupling limit one can transform intrinsic quadrupole moment to the laboratory frame in a simple way:

$$Q_{20}^{ex/gs}(exp) = \frac{3K^2 - I(I+1)}{(I+1)(2I+3)} Q_{20}^{ex/gs}, \quad (4)$$

where  $K$  is the projection of  $I$  on the (intrinsic) symmetry axis.

The calculated differences in the quadrupole moment between a given high- $K$  state ( $Q_{20}^{ex}$ ) and the ground state ( $Q_{20}^{gs}$ ):

$$\Delta Q_{20} = Q_{20}^{ex} - Q_{20}^{gs}, \quad (5)$$

are shown in Fig. 11 and Fig. 12, for No and Rf isotopes, respectively. Here and in the next subsection, the chosen states are marked in the same way:  $\pi^28^-$  by red dots,  $\nu^28^-$  by blue squares, and  $\pi^2\nu^216^+$  by green triangles. The dependence of  $\Delta Q_{20}$  vs  $N$  of excited neutron configuration is very similar in both elements, unlike for the

proton configuration. Quadrupole moments of excited proton configurations are bigger than in the ground state in Rf nuclei, while the difference is negative in No nuclei. As expected, with the fixed number of protons,  $\Delta Q_{20}$  for  $\pi^28^-$  states does not show a strong dependence on  $N$ . In the lightest isotopes, the two-quasineutron state has the largest difference  $\Delta Q_{20}$ , while  $\Delta Q_{20}$  turns negative for the heaviest shown isotopes. However, the most spec-

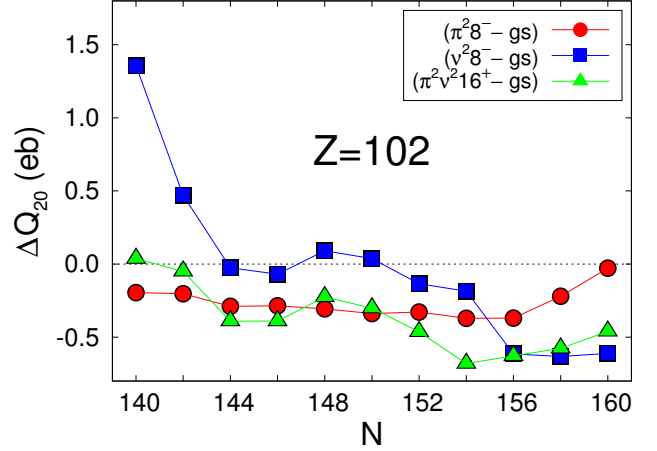


FIG. 11: The changes of the electric quadrupole moments in case of selected 2- and 4-qp configurations in No isotopes. Configurations:  $\pi^28^- = \{\pi 7/2^- [514] \otimes \pi 9/2^+ [624]\}$ ,  $\nu^28^- = \{\nu 7/2^+ [624] \otimes \nu 9/2^- [734]\}$ ,  $\pi^2\nu^216^+ = \{\pi^28^- \otimes \nu^28^-\}$ . The lines are drawn to guide an eye.

tacular differences  $\Delta Q_{20}$  we observe for the considered four-quasiparticle state  $\pi^2\nu^216^+$  (green colour). In most of No nuclei, the calculated  $Q_{20}$  is smaller in the excited state while for Rf nuclei the high- $K$  state is predicted to have larger  $Q_{20}$ . The difference  $\Delta Q_{20}$  is the largest for the lightest Rf isotopes, especially in  $^{244}\text{Rf}$ .

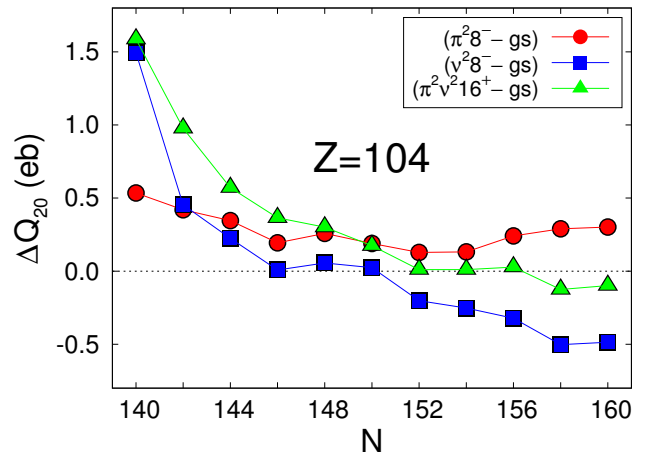


FIG. 12: The same as in Fig. 11, but in Rf isotopes.

### E. Mean-square charge radii

The mean-square charge radius:  $\langle r^2 \rangle$  characterizes the size of a nucleus. It is extracted from the measured atomic hyperfine structure which is determined by analysing atomic hyper - fine transitions. This structure is very sensitive to even slight changes in  $\langle r^2 \rangle$ , in particular those resulting from shape changes. The droplet model - like expression for  $\langle r^2 \rangle$  consists of four terms [48, 49]:

$$\langle r^2 \rangle = \langle r^2 \rangle_u + \langle r^2 \rangle_r + 3\sigma^2 + s_p^2, \quad (6)$$

where:  $\langle r^2 \rangle_u$  is the "uniform" term;  $\langle r^2 \rangle_r$  is the "Coulomb redistribution" term;  $3\sigma^2$  comes from the diffuseness of the nuclear surface and  $s_p^2$  is the finite-proton-size contribution. Interesting for us will be the difference in  $\langle r^2 \rangle$  between the high-K configuration and the spherical shape of a given nucleus:

$$\delta\langle r^2 \rangle = \langle r^2 \rangle_{def} - \langle r^2 \rangle_{sph}, \quad (7)$$

where  $\langle r^2 \rangle_{def}$  corresponds to deformation. According to this definition,  $\delta\langle r^2 \rangle$  can be understood as a measure of deviation from the spherical shape, characterized in (7) by  $\langle r^2 \rangle_{sph}$ .

We are going to discuss in this section isotopic dependance of  $\delta\langle r^2 \rangle$  not only for the ground states, but rather for selected multi-qv excited high-K configurations in relation to the ground states. A difference in  $\delta\langle r^2 \rangle$  between ground and excited states is:

$$\Delta\delta\langle r^2 \rangle = \delta\langle r^2 \rangle^{ex} - \delta\langle r^2 \rangle^{gs}, \quad (8)$$

In this difference, the last two components of Eq. 6 cancel. The Coulomb redistribution term  $\langle r^2 \rangle_r$ , which can be evaluated according to formula (23) in [48] is already a small quantity compared to  $\langle r^2 \rangle_u$ . It seems that the influence of the Coulomb redistribution effect on the difference (Eq. 8) may be neglected.

Thus, using all obtained deformations  $\beta_{\lambda 0}$  listed in (1) one can calculate  $\delta\langle r^2 \rangle \simeq \delta\langle r^2 \rangle_u$  (in a quite general way, see [50]) separately for deformed ground states (gs) and excited states (ex), as:

$$\delta\langle r^2 \rangle^{ex/gs} = \langle c^2 R_0^2 \rangle^{ex/gs} \cdot \left[ 1 + \frac{5}{4\pi} \sum_{\lambda=2,4,6,8} \beta_{\lambda 0}^2 \right]. \quad (9)$$

Seemingly, the changes of  $\delta\langle r^2 \rangle$  are very small, usually they are of the order of a few percent, but are measurable. For example, a relative change in mean-square charge radius due to one neutron less from the isotope shift can be estimated (in the spherical case), as:  $\delta\langle r^2 \rangle_{sph}^{A,A-1} / \delta\langle r^2 \rangle_{sph} = 1/(3A)$ , see [50], what means for a very heavy nuclei - considered here ( $A \approx 250$ ) about 0.1 percent. Now the need for a detailed analysis of the deformation parameters made in the previous paragraph becomes quite clear.

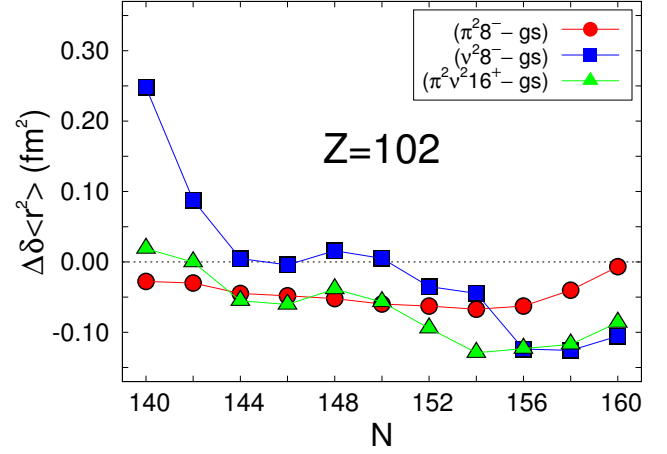


FIG. 13: The changes in mean-square nuclear charge radii  $\delta\langle r^2 \rangle$  for the selected 2- and 4-qv configurations in No isotopes. Configurations:  $\pi^2 8^- = \{\pi 7/2^- [514] \otimes \pi 9/2^+ [624]\}$ ,  $\nu^2 8^- = \{\nu 7/2^+ [624] \otimes \nu 9/2^- [734]\}$ ,  $\pi^2 \nu^2 16^+ = \{\pi^2 8^- \otimes \nu^2 8^-\}$ . The lines are drawn to guide an eye.

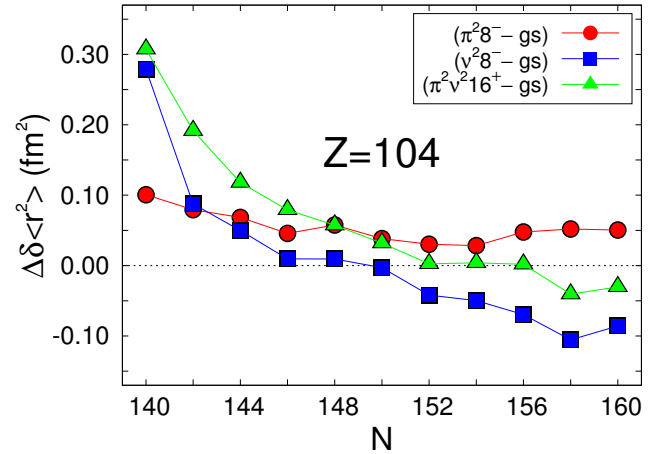


FIG. 14: The same as in Fig. 13, but in Rf isotopes.

The results based on definition 8 are shown in Figs. 13, 14.

One can assume that the size of a given nucleus at the spherical shape for both configurations (gs and ex) is the same:  $\langle c^2 R_0^2 \rangle^{gs} = \langle c^2 R_0^2 \rangle^{ex}$ , and than one can rewrite Eq. 8 in the explicit form:

$$\Delta\delta\langle r^2 \rangle = R_0^2 \frac{5}{4\pi} \sum_{\lambda=2,4,6,8} \langle \beta_{\lambda 0}^2 \rangle^{ex} - \langle \beta_{\lambda 0}^2 \rangle^{gs}. \quad (10)$$

However, we prefer to discuss numerical results with the properly calculated volume coefficient  $c$  in radius expansion.

Looking at Figs. 13, 14, one can see that the results for charge radii imitate those obtained for quadrupole moments, for all three states considered here. In principle, everything that has been said about  $\Delta Q_{20}$  vs  $N$  for these



states now can be repeated for  $\Delta\delta\langle r^2 \rangle$ . In particular, the behavior of both quantities in Rf and No for the corresponding high- $K$  states is similar. As before in the case of quadrupole moments, for configuration  $\pi^2\nu^216^+$  the dominant contribution to the observable effect in  $\Delta\delta\langle r^2 \rangle$  comes from the two-quasiparticle neutron excitation. One can clearly see that the plot for the neutron configuration is quite similar to that for the 4-qp excitation.

Finally, we would like to note that the calculated changes in the size-shape quantities are the smallest wherever the  $K$ -isomer is most likely. For example,  $\nu^28^- = \{\nu 7/2^+[624] \otimes \nu 9/2^-[734]\}$  state, suspected to be isomeric in  $^{252}\text{No}$  [38, 51, 52] or/and in  $^{254}\text{Rf}$  [44, 53], that is supported here by Figs.: 1, 2, 3, does not show almost any change of shape relative to the g.s. It is not surprising, as isomers occur where the excitation energy is relatively low. This means that the metastable minimum is slightly above the global minimum. The proximity of these minima means that the deformations for excited states are similar to those for the g.s. Consequently, the quantities such as  $Q_{20}$  and  $\delta\langle r^2 \rangle$  do not differ much from those for the g.s. In a sense, the lack of change of the nuclear shape in isomers may be just an indicator of their isomeric nature.

#### IV. CONCLUSIONS

We have shown on selected examples how the size of the very heavy nuclear system changes if one excited it. Such a studies seems are of particular importance for nuclei in which such states may have an isomeric character as they may be relatively long lived. After discussing the quality of our results with existing experimental data for

excitation energy we have indicated from isotopic chains such candidates. They are particularly clearly visible for  $N = 150$ , i.e. for:  $^{252}\text{No}$  and  $^{254}\text{Rf}$ , in all cases of considered multi-quasiparticle configurations.

Calculated charge radii and quadrupole moments for such excited states are compared with results for the ground states. The most pronounced difference in the behavior between nobelium and rutherfordium isotopes in excited states was observed for the considered four-quasiparticle configuration  $\pi^2\nu^216^+$  build on two-quasiproton:  $\{\pi 7/2^-[514] \otimes \pi 9/2^+[624]\}$  and two-quasineutron:  $\{\nu 7/2^+[624] \otimes \nu 9/2^-[734]\}$  excitations.

Also for those 4-qp configurations electric quadrupole moments and charge radii differ most significantly with the values of ground states.

Admittedly, for some high- $K$  states, the shape changes found are significant, but just for those suspected of isomerism they are rather negligible and this lack of shape change may just indicate on the isometric nature of the studied nuclear system.

The leading role of quadrupole deformation was shown and the impact of other shape parameters was discussed in details.

Since, the investigated No and Rf isotopes are not too far away from today's possibilities of experimental laser spectroscopy techniques above hypothesis and predictions for high- $K$  states may be verify soon.

#### ACKNOWLEDGEMENTS

M. K. was co-financed by the National Science Centre under Contract No. UMO-2013/08/M/ST2/00257 (LEA COPIGAL).

- 
- [1] H. J. Kluge, W. Nörtershäuser, *Spectrochimica Acta Part B, Atomic Spectroscopy*, **58**, no. 6, 1031 (2003).
  - [2] Yu. Gangrsky, *Hyperfine Interact.* **171**, 203 (2006).
  - [3] H. Backe, W. Lauth, M. Block, M. Laatiaoui, *Nuclear Physics A*, **944** 492 (2015).
  - [4] P. Campbell, I. D. Moore, M. R. Pearson, *Progress in Particle and Nuclear Physics*, **86** 127 (2016).
  - [5] M. Laatiaoui, W. Lauth, H. Backe, M. Block, D. Ackermann, B. Cheal, P. Chhetri, C. E. Düllmann, P. van Duppen, J. Even, et al., *Nature (London)*, **538**, 495 (2016).
  - [6] T. Murbüch, S. Raeder, P. Chhetri, K. Diaz, M. Laatiaoui, F. Giacoppo, M. Block, *Hyperfine Interactions* **241**, Article number: 35 (2020).
  - [7] S. Raeder et al., *Phys. Rev. Lett.* **120**, 232503 (2018).
  - [8] N. Boos et al., *Phys. Rev. Lett.* **72**, 2689 (1994).
  - [9] D. Ackermann, *Nucl. Phys A* **944**, 376 (2015).
  - [10] M. Asai, F. P. Heßberger, A. Lopez-Martens, *Nucl. Phys A* **944**, 308 (2015).
  - [11] Ch. Theisen, P. T. Greenlees, T. L. Khoo, P. Chowdhury, T. Ishii, *Nuclear Physics A* **944** 333 (2015).
  - [12] G. D. Dracoulis, P. M. Walker and F. G. Kondev, *Rep. Prog. Phys.* **79**, 076301 (2016).
  - [13] P. Walker and Z. Podolyák, *Phys. Scr.* **95**, 044004 (2020).
  - [14] P. M. Walker and F. R. Xu, *Phys. Scr.* **91**, 013010 (2016).
  - [15] P. T. Greenlees et al., *Phys. Rev. C* **78**, 021303(R) (2008).
  - [16] P. Jachimowicz, M. Kowal, and J. Skalski, *Phys. Rev. C* **98**, 014320 (2018).
  - [17] P. Jachimowicz, M. Kowal, and J. Skalski, *Phys. Rev. C* **92**, 044306 (2015).
  - [18] V. M. Strutinski, *Sov. J. Nucl. Phys.* **3**, 449 (1966), *Nucl. Phys. A* **95**, 420 (1967).
  - [19] S. Ówiok, J. Dudek, W. Nazarewicz, J. Skalski and T. Werner, *Comput. Phys. Commun.* **46**, 379 (1987).
  - [20] H. J. Krappe, J. R. Nix and A. J. Sierk, *Phys. Rev. C* **20**, 992 (1979).
  - [21] I. Muntian, Z. Patyk and A. Sobieczewski, *Acta Phys. Pol. B* **32**, 691 (2001).
  - [22] M. Kowal, P. Jachimowicz, A. Sobieczewski, *Phys. Rev. C* **82**, 014303 (2010).
  - [23] M. Kowal, J. Skalski, *Phys. Rev. C* **82**, 054303 (2010).
  - [24] M. Kowal, P. Jachimowicz, J. Skalski, arXiv:1203.5013 (2012).
  - [25] M. Kowal, J. Skalski, *Phys. Rev. C* **85**, 061302(R) (2012).
  - [26] P. Jachimowicz, M. Kowal, J. Skalski, *Phys. Rev. C* **85**,

- 034305 (2012), *Phys. Rev. C* **101**, 014311 (2020).
- [27] P. Jachimowicz, M. Kowal, J. Skalski, *Phys. Rev. C*, 044308 (2013).
- [28] P. Jachimowicz, M. Kowal, J. Skalski, *Phys. Rev. C* **89**, 024304 (2014).
- [29] P. Jachimowicz, M. Kowal, and J. Skalski, *Phys. Rev. C* **95**, 034329 (2017).
- [30] P. Jachimowicz, M. Kowal, and J. Skalski, *Phys. Rev. C* **95**, 014303 (2017).
- [31] A. Ghiorso et al., *Phys. Rev. C* **7**, 2032 (1973).
- [32] S. K. Tandel et al., *Phys. Rev. Lett.* **97**, 082502 (2006).
- [33] R. D. Herzberg et al., *Phys. Rev. Lett.* **97**, 082502 (2006).
- [34] R. D. Herzberg, et al., *Nature*, **442**, 996 (2006).
- [35] F. P. Heßberger et al., *Eur. Phys. J. A* **43**, 55 (2010).
- [36] R. M. Clark et al., *Phys. Lett. B* **690**, 19 (2010).
- [37] A.P. Robinson, et al., *Phys. Rev. C* **78**, 034308 (2008).
- [38] B. Sulignano, et al., *Phys. Rev. C* **86**, 044318 (2012).
- [39] F.G. Kondev, et al., in: *Proceeding of the International Conference on Nuclear Data for Science and Technology, EDP Sciences*, (2007).
- [40] R. V. Jolos, L. A. Malov, N. Yu. Shirikova and A. V. Sushkov *J. Phys. G: Nucl. Part. Phys.* **38**, 115103 (2011).
- [41] J. Kallunkathariyil et al., *Phys. Rev. C* **101**, 011301(R) (2020).
- [42] D. Peterson et al., *Phys. Rev. C* **74**, 014316 (2006).
- [43] H. L. Liu, P. M. Walker, and F. R. Xu, *Phys. Rev. C* **89**, 044304 (2014).
- [44] H.M. David, et al., *Phys. Rev. Lett.* **115**, 132502 (2015).
- [45] Z. Patyk, A. Sobiczewski, *Nuclear Phys. A* **533**, 132 (1991).
- [46] Z. Patyk, A. Sobiczewski, *Phys. Lett. B* **256**, 307 (1991).
- [47] H. L. Liu, F. R. Xu, P. M. Walker, and C. A. Bertulani, *Phys. Rev. C* **83**, 011303(R) (2011).
- [48] W. D. Myers, K-H Schmidt, *Nuclear Physics A* **410**, 61-73 (1983).
- [49] F. Buchinger et al., *Phys. Rev. C* **49**, 3 (1994).
- [50] Ch. Scheidenberger (Editor), M. Pfützner (Editor), *The Euroscool on Exotic Beams, vol. IV*, Springer-Verlag Berlin and Heidelberg GmbH & Co., (2014).
- [51] R. D. Herzberg, et al., *Phys. Rev. C* **65**, 014303 (2001).
- [52] A. P. Leppänen, et al., *Eur. Phys. J. A* **28**, 301 (2006).
- [53] J.Khuyagbaatar, et al., *Nuclear Physics A* **994**, 121662 (2020).